Journal of Applied Polymer Science

Towards enhanced electrochemical capacitance with self-assembled synthesis of poly(pyrrole-*co*-*o*-toluidine) nanoparticles

Zhenzhong Hou, Qinghao Yang, Hai Lu, Ying Li
College of Material Science and Engineering, Xi'an University of Science and Technology, Xi'an 710054, People's Republic of China
Correspondence to: Z. Hou (E-mail: hzzhong1981@yeah.net)

ABSTRACT: Poly(pyrrole-*co*-*o*-toluidine) (PPOT) nanoparticles for electrochemical capacitors are easily and productively synthesized by a chemical oxidative polymerization of pyrrole (PY) and *o*-toluidine (OT) in 0.5*M* HCl without any external additive. The polymerization yield, electrical conductivity, and size of the copolymer nanoparticles can significantly be optimized by the oxidant/monomer molar ratio and polymerization temperature. The chemical structure of the obtained copolymer is characterized by UV–vis and FTIR. The copolymer nanoparticles synthesized at 10°C are found to generally have irregular granular morphology with a diameter of 60–100 nm and a small polydispersity index of 1.06 by laser particle-size analyzer, FE-SEM, and TEM, and good dispersibility in water. The formation mechanism of the nanoparticles is proposed based on the powerful amphipathicity from comonomer aggregate formed by PY and OT in the monomer solution. The PPOT nanoparticles possess a specific capacitance of 310 F g^{-1} at 25 mV s^{-1} as well as retain 81% of the initial specific capacitance value after 1000 cycles, while its energy density and power density are found to be 40.2 and 1196 W Kg^{-1} at 2 A g^{-1}. The enhanced electrochemical properties can be attributed to the nanostructural advantage of the PPOT. © 2015 Wiley Periodicals, Inc. J. Appl. Polym. Sci. **2016**, *133*, 42995.

KEYWORDS: copolymer nanoparticles; o-toluidine; pyrrole; self-assembly; specific capacitance

Received 10 March 2015; accepted 28 September 2015
DOI: 10.1002/app.42995

INTRODUCTION

Conducting polymers have received considerable attention for potential application in electrochemical supercapacitors because they possess many advantages of low cost and environmental impact, high charge density, high voltage window, and adjustable redox activity.[1,2] PPY of conducting polymers is the most attractive one, as a supercapacitor or battery electrode, due to its more flexibility in electrochemical processing.[3] Unfortunately, swelling and shrinking of conducting polymers caused by the intercalating/deintercalating (redox) process often lead to mechanical degradation of the conducting polymer-based electrodes, significantly fading their electrochemical performance during cycling. It was reported that, at a constant current density of 2 mA cm^{-2}, the capacitance of the PPY electrodes-formed electrochemical supercapacitor device was reduced by 50% in the first 1000 cycles (the initial capacitance is 120 F g^{-1}).[4] Furthermore another disadvantage of the dense growth makes PPY low ion accessibility, which hinders its electrochemical properties, especially for the thicker films or coatings.[5]

One developing way to mitigate the low cycling stability is preparing nanostructured conducting polymers such as nanofibers/wires, nanotubes, nanorods, nanospheres, and irregular nanoparticles. It seems that nanostructured conducting polymers could efficiently reduce the cycling degradation problem caused by volumetric changes, thus enhance the utilization of electrode materials. Ghamouss *et al.*[6] have synthesized PPY nanospheres with a diameter of around 60 nm in glycerol medium without external stabilizers at 0°C and attained the specific capacitance of 200.3 F g^{-1}, which had a improvement of about 30% compared with the conventional PPY particles. Wan *et al.* proposed a novel and simple self-assembly approach named template-free method to prepare nanostructured conducting polymers through the micelles formed by dopant and/or monomer-dopant in reaction systems guiding the polymerization.[7–13] Nevertheless, this method needs special dopants, such as organic carboxylic acids,[9] naphthalene sulfonic acids,[10] molybdic acid,[11] azobenzene sulfonic Acid,[12] etc., to achieve the self-assembly process. On this basis, a more facile template-free way has been developed to synthesize pyrrole (PY) and aniline copolymer nanoparticles.[14–18] In the self-assembled formation mechanism in this approach "electrostatic interaction" and/or "amphipathicity" of comonomers are the driving force of forming conducting copolymer nanoparticles.

As an aniline derivative, OT is an appropriate monomer to be copolymerized with PY to synthesize poly(pyrrole-*co*-*o*-toluidine) (PPOT) nanoparticles due to its amphiphilic structure with hydrophilic —NH_2 and hydrophobic —C_7H_7. Furthermore, introducing OT units into PPY may improve some of its properties, especially the electrochemical capacitance. However, the investigations about this novel copolymer are so rare. Li *et al.* have synthesized the soluble copolymer of PY-OT by chemical synthesis technique and studied the effect of PY/OT molar ratio on the yield, intrinsic viscosity, and solubility of the copolymers.[19] Yalçinkaya *et al.* have reported that PPOT film could be deposited on mild steel surface through electrochemical polymerization in oxalic acid solution.[20] They also synthesized highly stable and extremely thin poly(pyrrole-*co*-*o*-anisidine-*co*-*o*-toluidine) film (0.80 μm).[21] The copolymer exhibited excellent anti-corrosion performance due to its high stability, high adhesion and low permeability. Unfortunately, only these reports focus on the solubility and corrosion resistance of copolymers, but their electrochemical capacitance is neglected. In this work, we have firstly prepared PPOT nanoparticles via self-assembled copolymerization of PY and OT in aqueous solution without any external additive. The structure, morphology and electrochemical capacitance of PPOT nanoparticles and their formation mechanism through a self-assembly were also investigated and revealed in detail.

EXPERIMENTAL

Materials

PY monomer was purchased from Sinopharm Chemical Reagent and distilled under reduced pressure before use. OT, ammonium persulfate (APS), hydrochloric acid, and ethanol were of analytical grade and used as received (Tianjin Chenfu Chemical Reagent Company, China).

Synthesis

A typical synthetic route was as follows: PY (6 mmol) and OT (4 mmol) were dissolved in HCl solution (0.5*M*, 100 mL) under magnetic stirring at 10°C for half an hour. APS as an oxidant was dissolved in HCl (0.5*M*, 20 mL) solution at the same temperature. Then the APS solution was added into the above monomer mixture in one portion under magnetic stirring. Copolymerization was carried out for 8 h at 10°C in air. The as-prepared products were obtained by centrifugation, and then washed with ethanol and deionized water for several times until the upper layer liquid became colorless. Finally, the black polymer powder was dried in a vacuum oven at 60°C for 24 h.

Characterization

Fourier transform infrared (FTIR) spectrum was recorded on a Bruker FTIR Equinox 55 spectrophotometer using KBr pellets. UV–vis spectrum of the copolymer in DMSO was measured on a 760CRT spectrophotometer (Precision and Scientific Instrument Corporation, Shanghai, China) at a scanning rate of 400 nm min^{-1}. The size and its distribution of PPOT particles were analyzed by an LS230 laser particle-size analyzer (LPA) from Beckman Coulter. The real size and morphology of PPOT nanoparticles were observed by a FE-SEM (ZESIS SIGMA, Germany) and a TEM (Hitachi Model H800, Japan). The electrical conductivities of pressed PPOT round-shaped pellets with the thickness of about 3 mm and diameter of 1.5 cm were examined by a four probe technique at room temperature with a SDY-4 digital four-probe meter (Guangzhou, China). Electrochemical performance of the PPOT sample was evaluated by cyclic voltammetry (CV), galvanostatic charge/discharge (GCD) and electrochemical impedance spectroscopy (EIS), which were performed on CS 350 electrochemical workstation (Corrtest Corporation, Wuhan China) at room temperature. All electrochemical experiments were carried out in 1*M* $NaNO_3$ aqueous solution using a three-electrode system, which contained a saturated calomel electrode and a platinum plate (ca. 1 cm^2) as the reference electrode and counter electrode, respectively, the obtained PPOT loaded on foam nickel as the working electrode. (Working electrodes were prepared by mixing 85 wt % as-prepared PPOT with 10 wt % acetylene black and 5 wt % polytetrafluoroethylene dissolved in ethanol as a binder to form a homogeneous slurry. The obtained slurry was then pressed onto a foam nickel (1 cm^2) at 5 MPa for 1 min and dried under vacuum at 60°C for 24 h. The dried electrode can generally hold around 5 mg of as-prepared polymers.)

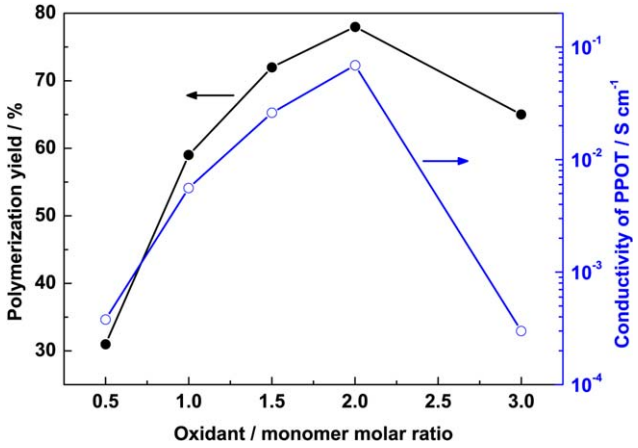

Figure 1. Polymerization yield and electrical conductivity of PPOT particles synthesized at different oxidant (APS)/monomer molar ratios at 10°C for 8 h. [Color figure can be viewed in the online issue, which is available at wileyonlinelibrary.com.]

RESULTS AND DISCUSSION

Synthesis

The effect of oxidant/monomer molar ratio on the yield and conductivity of PPOT synthesized at 10°C has been described in Figure 1. The maximum yield 78% and conductivity 6.9 × 10^{-2} S cm^{-1} appear at the oxidant/monomer molar ratio of 2 at the same time. When less oxidant is added, enough monomer cation-radicals or active sites cannot form due to the quick consumption of oxidant, leading to an inadequate polymerization and lower oxidized-state content,[15] followed by the simultaneous decrease in the yield and conductivity. On the contrary, excess oxidant may cause overoxidation, even decomposition of the polymer chains, unavoidably lowering the yield and conductivity. Therefore, the optimal oxidant/monomer molar ratio is 2 for the synthesis of PPOT with high yield and conductivity.

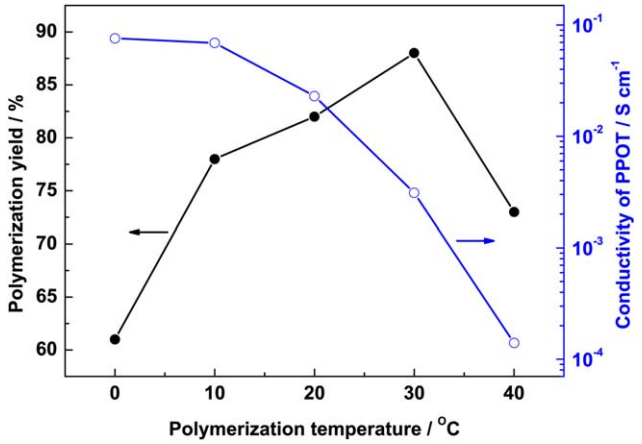

Figure 2. Polymerization yield and electrical conductivity of PPOT particles synthesized at different temperatures at a constant APS/monomer molar ratio of 2 for 8 h. [Color figure can be viewed in the online issue, which is available at wileyonlinelibrary.com.]

Figure 2 presents the plots of the yield and conductivity of PPOT as a function of polymerization temperature, displaying the maximum yield and conductivity at 30 and 0°C respectively in a temperature range between 0 and 40°C. As we all know, more α-α couplings between PY monomers occur during the copolymerization with OT comonomers at lower temperature because of a controllable copolymerization,[22] which significantly elevates the conjugation and thereby the conductivity. However, too low a temperature would reduce reactivity of monomers, decreasing the polymerization yield. On the other hand, too high temperature might induce more structure/conformation defects with a poor conjugation. Besides, it is difficult to obtain PPOT nanoparticles above 20°C because of faster and more drastic polymerization rate elevating the "overgrowth" of copolymer at an higher temperature.[23,24] The comprehensive analysis indicates that 10°C is the optimal temperature for the preparation of PPOT nanoparticles with relatively high yield and conductivity.

Spectroscopic Characterization

Representative FTIR spectra for PPY, PPOT, and POT [poly(*o*-toluidine)] are shown in Figure 3(a). For the POT [spectrum *A* in Figure 3(a)], the two bands appearing at about 1590 and 1495 cm^{-1} correspond to the stretching vibration of the quinoid and benzenoid ring units, respectively.[25] The band at 1372 cm^{-1} is due to the symmetric deformation of methyl group.[26] The peaks at around 1317 and 1213 cm^{-1} can be assigned to the C—N stretching mode, whereas the peaks at 1155, 1113, and 1007 cm^{-1} are the characteristic bands of C—H vibration.[25,27,28] The three bands centered at 940, 882, and 813 cm^{-1} can be characterized to an in-plane C—H vibration of quinoid rings, 1,2,4-substitution in the benzenoid rings, and an out-of-plane C—H vibration.[28] As for the PPY [spectrum *C* in Figure 3(a)], the two peaks at 1543 and 1453 cm^{-1} can be attributed to the asymmetric and symmetric stretching vibrations of PY rings, respectively.[29] The band at about 1305 cm^{-1} is ascribed to the C—N stretching in PY units.[30] The obvious peak at 1183 cm^{-1} reflect the C—H stretching of PY rings, while the peaks of C—H deformation vibrations appear at 1040 and 910 cm^{-1}.[31,32] According to the above analysis, it can be found from Figure 3(a) that the PPOT spectrum has the characteristic bands of both PPY and POT. The broad peaks (a) between 1500 and 1700 cm^{-1} correspond to stretching vibrations of PY and benzenoid rings. The peak (b) at about 1384 cm^{-1} can be attributed to methyl groups of the OT units in the polymer chains, while the four bands (c, d, e, and f) at 900–1250 cm^{-1} reflect C—N and C—H vibrations of PY and OT units. In addition, the bands around 1007–1040 cm^{-1} in all spectra of the polymers not only correspond to C—H vibrations but also ascribe S=O stretching vibrations from APS.[17,25] A comparison of the spectra of POT, PPY, and PPOT exhibits some differences in the relative absorbance and wavenumber, revealing the obtained PPOT is a real copolymer containing PY and OT units.

The UV–vis absorption spectrum of PPOT salts in DMSO in Figure 3(b) shows two bands: the strong band 1 around 310 nm due to π-π^* transition of aromatic rings in copolymer chains;

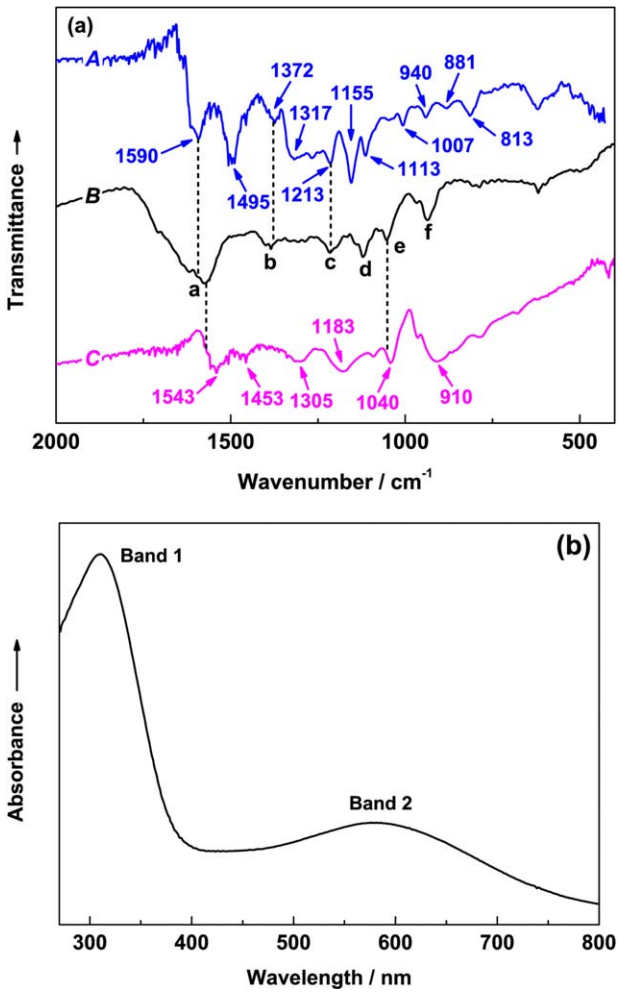

Figure 3. (a) FTIR spectra of the polymers synthesized at APS/monomer molar ratio of 2 for 8 h at 10°C: (A) POT; (B) PPOT; (C) PPY; (b) UV–vis spectrum of PPOT synthesized at APS/monomer molar ratio of 2 for 8 h at 10°C. [Color figure can be viewed in the online issue, which is available at wileyonlinelibrary.com.]

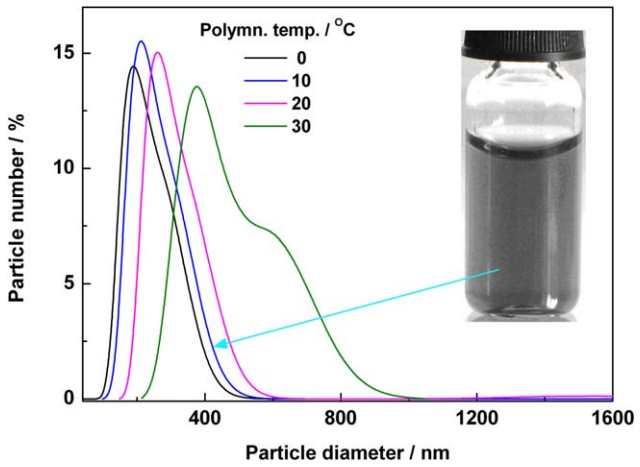

Figure 4. Size distribution in pure water of PPOT particles synthesized at different temperatures from 0 to 30°C for 8 h with APS/monomer molar ratio of 2. Inset: aqueous dispersion of the PPOT particles synthesized at 10°C. [Color figure can be viewed in the online issue, which is available at wileyonlinelibrary.com.]

the broad band 2 with peak at about 580 nm owing to the n-π^* transition of large π conjugated system of the copolymer.[33–35] Pure PPY is hardly soluble in most organic solvents including DMSO, while the copolymer exhibits improved solubility. As a result, the UV–vis spectrum of copolymer could reflect electron transition of "the whole copolymer chain," suggesting that the PPOT has large π-conjugation and thus relatively good conductivity.

Size and Morphology Characterization

LPA reveals that polymerization temperature has a significant influence on the size of PPOT particles, as shown in Figure 4. With elevating polymerization temperature from 0 to 30°C, the PPOT particle size and its distribution gradually increase, demonstrating the smallest size and the narrowest size distribution simultaneously at 0°C. More drastic polymerization with higher growth rate at the higher temperature of 30°C will make the as-formed particles conglomerate. A similar result has be found for the copolymerization of aniline and 5-sulfonic-2-anisidine.[15] Unfortunately, the PPOT sample synthesized at 0°C shows the lowest yield (Figure 2), so we choose the copolymer sample, obtained at 10°C, with the D_n 231 nm and polydispersity index (D_w/D_n) 1.06 as a research object owing to its obviously improved yield and relatively small size. In addition, the picture of the aqueous dispersion of the PPOT particles formed at 10°C has been observed in Figure 4, inset. It can be seen that the dispersion seems rather uniform, just like a homogeneous solution, substantially signifying nano-sized copolymer particles because of their complete insolubility in water. Note that the particle diameter measured by LPA is not the real size but just the apparent diameter due to the swelling effect, so the real size of PPOT particles would be much smaller, just like that shown from the following SEM and TEM observation.

It is seen from Figure 5 that the PPOT particles synthesized at 10°C without using any templates and surfactants indeed have a nanoscale size, about 30–110 nm [Figure 5(b)], while the pure PPY synthesized at the same conditions exhibits typical potato-like particles with a size above 300 nm [Figure 5(a)]. Most of the PPOT particles usually have a diameter of 60–100 nm, which can be revealed by TEM [Figure 5(c)]. Furthermore, the nanoparticles exhibit an irregular granular morphology, which can provide larger specific surface area than the regular sphere as well as higher porous structure than dense bulk PPY.[4] Therefore, the PPOT nanoparticles could be used as electrode materials with enhanced electrochemical capacitance for supercapacitor application.

Formation Mechanism

A possible mechanism for the formation of PPOT nanoparticles is given in Figure 6, which could be described as the atypical "micelle soft template" self-assembly mechanism. In our case, with dissolving PY and OT in the HCl solution, the neighboring PY and OT monomers can aggregate gradually with each other due to the balance between central hydrophobic core and outer hydrophilic $-NH_2$ groups, forming an internally hydrophobic but externally hydrophilic co-monomer aggregate containing neutral PY monomers inside. Moreover, the π-π interaction between protonated PY and comonomer as well as possible hydrogen bonding interaction could promote the formation of above-mentioned comonomer aggregate. After adding the oxidant, the polymerization will naturally occur inside each

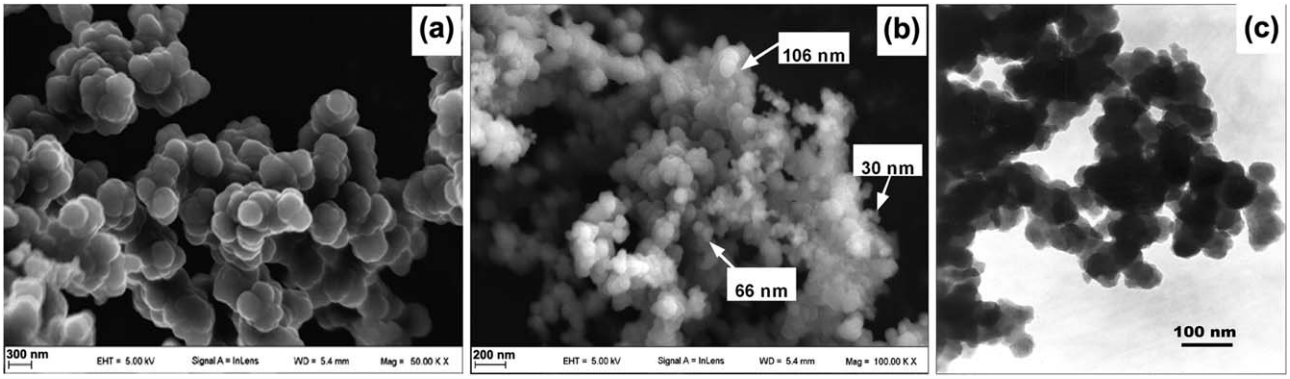

Figure 5. FE-SEM (a,b) and TEM (c) images of PPY (a), PPOT (b,c). All the polymers were synthesized at 10°C with APS/monomer molar ratio of 2 for 8 h.

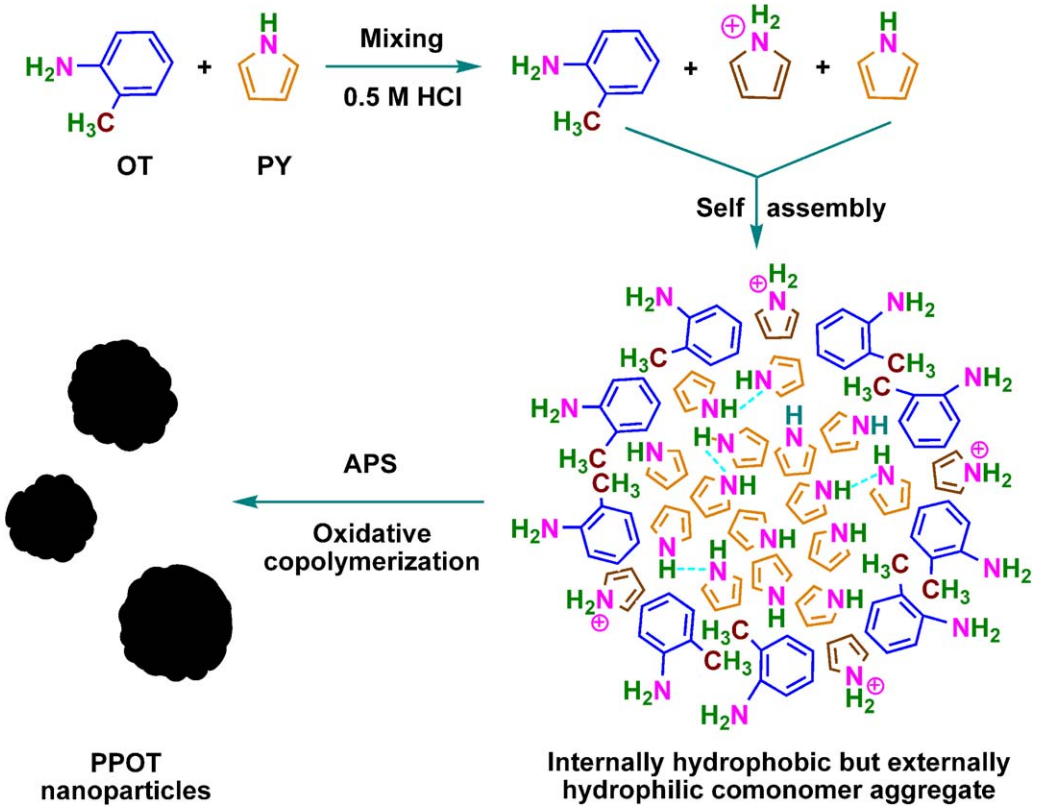

Figure 6. Formation mechanism of the PPOT nanoparticles through a self-assembly. [Color figure can be viewed in the online issue, which is available at wileyonlinelibrary.com.]

aggregate to form a granular nanoparticle at relatively low temperature. Finally, the PPOT nanoparticles with the diameter of 30–110 nm are achieved through some agglomeration in the synthetic process. We can say OT monomers play a key role in the formation of PPOT nanoparticles, which can be confirmed by the synthesized PPY at the same polymerization condition without OT having an particle size above 300 nm [Figure 5(a)]. Comparing with the classical "micelle soft template" self-assembly mechanism,[7–13,32,33,36] we here apply comonomer instead of the special dopants or oxidants to develop the micelle-like aggregate through a self-assembly.

Electrochemical Characterization

Figure 7(a) depicts the CV curves of PPY and PPOT electrodes in 1*M* $NaNO_3$ at 25 mV s^{-1}. The above two polymers have been prepared at the same polymerization condition. Obviously, both curves in this figure exhibit a typical faradaic capacitance performance, and the current response in the case of PPOT is significantly larger, indicating that PPOT electrode possesses better capacitance performance with symmetrical redox behavior than PPY electrode. The specific capacitances of PPY and PPOT can be calculated from CV curves, according to eq. (1)[6,37]

$$C = \int \frac{I}{vmV} dV \tag{1}$$

where C is the specific capacitance (F g^{-1}); I is the response current (A); m is the the mass of the electroactive material in the electrode (g); v is the potential scan rate (V s^{-1}) and V is the potential (V). The calculated specific capacitances of PPY and PPOT are 200 and 310 F g^{-1}, respectively.

However, the specific capacitance for PPOT can also be calculated from the GCD curve in Figure 7(a) inset by eq. (2)[38,39]

$$C = \frac{I \times \Delta t}{m \times \Delta V} \tag{2}$$

where C, I, m, Δt, and ΔV are the specific capacitance (F g^{-1}), the charge current (A), the mass of the electroactive material in the electrode (g), the charge time (s), and the voltage range (V), respectively. The PPOT electrode delivers a specific capacitance of 290 F g^{-1} at 2 A g^{-1}, while its energy density and power density are found to be 40.2 Wh Kg^{-1} and 1196 W Kg^{-1} by using the calculating ways described in Ref. 40.

Figure 7(b) shows the specific capacitance values of PPY and PPOT electrodes as a function of cycle numbers. It can be found from this figure that the electrode based on bulk PPY remarkably degrades during cyclic process, while the PPOT nanoparticles-based electrode exhibits good cycling life with slower descent speed in specific capacitance. The capacitance of PPY and PPOT retain about 54 and 81% after a thousand cycles. Nanosized PPOT particles inevitably enhance the active surface area of the electroactive material, consequently, facilitate ion diffusion and charge storage during the electrochemical reactions in the PPOT electrode, which is responsible for the higher capacitance and cycling stability.

EIS is a complementary technique that could further provide more information about the electrochemical behaviors of the PPY and PPOT electrodes. Typical Nyquist plots for PPY and PPOT electrodes at open circuit potentials are shown in Figure 8. The experimental results were fitted using an appropriate equivalent circuit and the electrical parameters found from fitting were tabulated (Figure 8 inset). In every plot, a single approximate semi-circle in the high frequency region and a straight line in the low frequency region are observed. The very high frequency intercept with the real axis is equal to the solution resistance (R_s) and the diameter of the semicircle indicates the charge transfer resistance (R_{ct}) of polymer. Two constant phase elements CPE1 and CPE2 are related to the double layer capacitance and the pseudocapacitance produced by ionic diffusion process in the electrode, respectively.[41] The parameter n has values that range from 0 to 1. $n = 1$ denotes the CPE element is an ideal capacitor, while $n = 0$ and 0.5, represents a resistance and Warburg behavior, respectively.[42,43] As seen from Figure 8 inset, the value of CPE2 is much larger than that of CPE1 in both PPOT and PPY electrodes, indicating that the main capacitance of the two electrodes arises from faradic pseudocapacitance. Moreover, PPOT electrode possesses a lower R_{ct} and a higher CPE2 as well as n_2 closer to 1 compared with PPY electrode, revealing its enhanced capacitive performance.

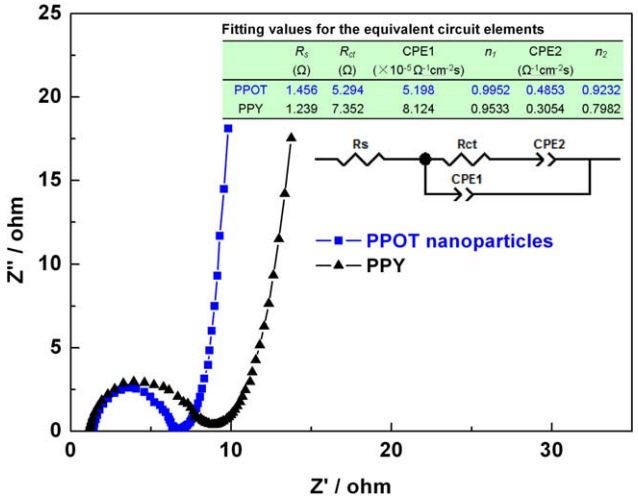

Figure 8. Nyquist plots of PPOT and PPY electrodes at open circuit potential in 1*M* $NaNO_3$ in the frequency range of 0.01–10^4 Hz. Inset: the equivalent circuit for the simulation of the experimental data and its corresponding electrical parameters list. [Color figure can be viewed in the online issue, which is available at wileyonlinelibrary.com.]

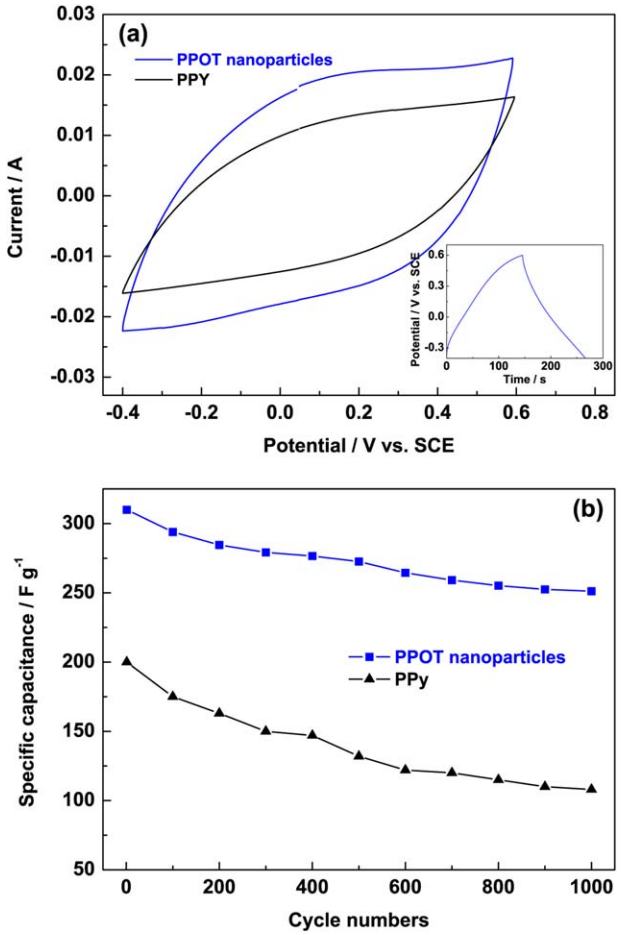

Figure 7. (a) CV curves of PPY, and PPOT nanoparticles electrodes in 1*M* $NaNO_3$ with a sweep rate of 25 mV s^{-1} at 25°C. Inset: GCD curve for PPOT nanoparticles at a current density of 2 A g^{-1}. (b) Cycling stability of synthesized PPY and PPOT electrodes with cycle numbers from 1 to 1000 in 1*M* $NaNO_3$ at 25 mV s^{-1} at 25°C. [Color figure can be viewed in the online issue, which is available at wileyonlinelibrary.com.]

CONCLUSIONS

The PPOT nanoparticles have been directly synthesized by a chemical oxidative polymerization of PY and OT in 0.5*M* HCl medium without any external stabilizer via self-assembled synthesis. Two fundamental polymerization parameter including oxidant/monomer molar ratio and polymerization temperature have been used to significantly optimize the yield, conductivity, and size of copolymer particles; 10°C with oxidant/monomer molar ratio of 2 are optimal copolymerization conditions for the synthesis of the PPOT nanoparticles with relatively high yield and conductivity. The obtained nanoparticles exhibit a irregular granular morphology with size of 60–100 nm and good dispersibility in water. As the electrode materials, the PPOT nanoparticles deliver a higher specific capacitance (310 F g^{-1} at 25 mV s^{-1}) and better electrochemical stability (the retention rate of specific capacitance is 81% after 1000 cycles) than PPY synthesized at the same conditions. These results indicate the copolymerization is an effective approach to synthesize novel conducting polymers with enhanced electrochemical performance for supercapacitor application.

ACKNOWLEDGMENTS

This work was financially supported by the National Nature Science Foundation of China (No. 21204072).

REFERENCES

1. Snook, G. A.; Kao, P.; Best, A. S. *J. Power Sources* **2011**, *196*, 1.

2. Wang, G.; Zhang, L.; Zhang, J. *Chem. Soc. Rev.* **2012**, *41*, 797.
3. Hughes, M.; Chen, G. Z.; Shaffer, M. S. P.; Fray, D. J.; Windle, A. H. *Compos. Sci. Technol.* **2004**, *64*, 2325.
4. Sharma, R. K.; Rastogi, A. C.; Desu, S. B. *Electrochim. Acta* **2008**, *53*, 7690.
5. Snook, G. A.; Best, A. S. *J. Mater. Chem.* **2009**, *19*, 4248.
6. Ghamouss, F.; Brugère, A.; Anbalagan, A. C.; Schmaltz, B.; Luais, E.; Tran-Van, F. *Synth. Met.* **2013**, *168*, 9.
7. Wan, M. X. *Adv. Mater.* **2008**, *20*, 2926.
8. Ding, H. J.; Long, Y. Z.; Shen, J. Y.; Wan, M. X. *J. Phys. Chem. B* **2010**, *114*, 115.
9. Zhang, L. J.; Long, Y. Z.; Chen, Z. J.; Wan, M. X. *Adv. Funct. Mater.* **2004**, *14*, 693.
10. Zhang, Z. M.; Wei, Z. X.; Zhang, L. J.; Wan, M. X. *Acta Mater.* **2005**, *53*, 1373.
11. Zhang, L. X.; Zhang, L. J.; Wan, M. X. *Eur. Polym. J.* **2008**, *44*, 2040.
12. Huang, K.; Wan, M. X. *Synth. Met.* **2003**, *135-136*, 173.
13. Long, Y. Z.; Li, M. M.; Gu, C. Z.; Wan, M. X.; Duvail, J. L.; Liu, Z. W.; Fan, Z. Y. *Prog. Polym. Sci.* **2011**, *36*, 1415.
14. Li, X. G.; Zhang, R. R.; Huang, M. R. *J. Comb. Chem.* **2006**, *8*, 174.
15. Li, X. G.; Lü, Q. F.; Huang, M. R. *Small* **2008**, *4*, 1201.
16. Li, X. G.; Wei, F.; Huang, M. R.; Xie, Y. B. *J. Phys. Chem. B* **2007**, *111*, 5829.
17. Li, X. G.; Hou, Z. Z.; Huang, M. R. *J. Phys. Chem. C* **2009**, *113*, 21586.
18. Lü, Q. F.; He, Z. W.; Zhang, J. Y.; Lin, Q. L. *J. Anal. Appl. Pyrolysis* **2012**, *93*, 147.
19. Li, X. G.; Wang, L. X.; Jin, Y.; Zhu, Z. L.; Yang, Y. L. *J. Appl. Polym. Sci.* **2001**, *82*, 510.
20. Yalçinkaya, S.; Tüken, T.; Yazici, B.; Erbil, M. *Prog. Org. Coat.* **2008**, *63*, 424.
21. Yalçinkaya, S.; Tüken, T.; Yazici, B.; Erbil, M. *Curr. Appl. Phys.* **2010**, *10*, 783.
22. Kros, A.; Nolte, R. J. M.; Sommerdijk, N. A. J. M. *Adv. Mater.* **2002**, *14*, 1779.
23. Huang, J. X.; Kaner, R. B. *Chem. Commun.* **2006**, *367*.
24. Liu, S. W.; Zhu, K. Z.; Zhang, Y.; Xu, J. R. *Polymer* **2006**, *47*, 7680.
25. Tursun, A.; Zhang, X. G.; Ruxangul, J. *J. Appl. Polym. Sci.* **2005**, *96*, 1630.
26. Zampronio, E. C.; Oliveira, H. P. *Meter. Res. Bull.* **2004**, *39*, 1525.
27. Milind, V. K.; Annamraju, K. V. *Eur. Polym. Mater.* **2004**, *40*, 379.
28. Fujita, I.; Ishiguchi, M.; Shiota, H.; Danj, T.; Kosai, K. *J. Appl. Polym. Sci.* **1992**, *44*, 987.
29. Liu, J.; Wan, M. X. *J. Mater. Chem.* **2011**, *11*, 404.
30. Shen, M.; Han, Y.; Lin, X.; Ding, B.; Zhang, L.; Zhang, X. *J. Appl. Polym. Sci.* **2013**, *127*, 2938.
31. Maity, A.; Sinha, R. S. *Macromol. Rapid Commun.* **2008**, *29*, 1582.
32. Rana, U.; Chakrabarti, K.; Malik, S. *J. Mater. Chem.* **2011**, *21*, 11098.
33. Shen, C.; Sun, Y.; Yao, W.; Lu, Y. *Polymer* **2014**, *55*, 2817.
34. Elmansouri, A.; Outzourhit, A.; Lachkar, A.; Hadik, N.; Abouelaoualim, A.; Achour, M. E.; Oueriagli, A.; Ameziane, E. L. *Synth. Met.* **2009**, *159*, 292.
35. Athawale, A. A.; Kulkarani, M. V.; Chabukswar, V. V. *Mater. Chem. Phys.* **2002**, *73*, 106.
36. Liu, Z.; Zhang, X.; Poyraz, S.; Surwade, S. P.; Manohar, S. K. *J. Am. Chem. Soc.* **2010**, *132*, 13158.
37. Yang, Q.; Hou, Z.; Huang, T. *J. Appl. Polym. Sci.* **2015**, *132*, 41615.
38. Liang, J.; Dong, B.; Ding, S.; Li, C.; Li, B. Q.; Li, J.; Yang, G. *J. Mater. Chem. A* **2014**, *2*, 11299.
39. Dong, B.; Zhang, X.; Xu, X.; Gao, G.; Ding, S.; Li, J.; Li, B. *Carbon* **2014**, *80*, 222.
40. Jin, Y.; Huang, S.; Zhang, M.; Jia, M. *Synth. Met.* **2013**, *168*, 58.
41. Guan, H.; Fan, L. Z.; Zhang, H.; Qu, X. *Electrochim. Acta* **2010**, *56*, 964.
42. Li, H.; Wang, J.; Chu, Q.; Wang, Z.; Zhang, F.; Wang, S. *J. Power Sources* **2009**, *190*, 578.
43. Ramya, R.; Sivasubramanian, R.; Sangaranarayanan, M. V. *Electrochim. Acta* **2013**, *101*, 109.